Path integral quantum algorithm for simulating non-Markovian quantum dynamics in open quantum systems

Peter L. Walters [1] and Fei Wang [1,2,*]

[1]*Department of Chemistry and Biochemistry, George Mason University, Fairfax, Virginia 22030, USA*
[2]*Quantum Science and Engineering Center, George Mason University, Fairfax, Virginia 22030, USA*

(Received 21 April 2023; accepted 2 January 2024; published 1 February 2024)

Research in open quantum system dynamics has received growing interest in recent years, and its ongoing investigation has uncovered many intriguing physics departing from closed systems. A particularly useful application of the open quantum system theory is to simulate quantum dynamical processes in condensed phase materials. As the quantum degree of freedom is constantly under the influence of its thermal environment, the accurate description of the dynamics often requires non-Markovian time evolution at finite temperature. Such calculation is usually quite challenging on classical computers as extensive memory storage is required. In this work, we focus on a quantum system linearly coupled to its harmonic bath and present a path integral based quantum algorithm that time-evolves the reduced density matrix under finite temperature non-Markovian dynamics. To treat the nonunitary time evolution, the Sz.-Nagy dilation scheme is used for the conversion to unitary dynamics that can be implementable on gate-based quantum computers. The modified Hadamard test is then used to retrieve all the information of the reduced density matrix. Complexity analysis shows that the memory requirement has exponential reduction on the quantum machine whereas the runtime complexity stays roughly the same as for the classical computer. It points to the possibility of using this algorithm to simulate multilevel and multisite non-Markovian quantum dynamics that are beyond the reach of classical computers. The algorithm makes no ad hoc assumptions and extends naturally beyond Markovian and weak coupling regimes. We validated the algorithm on the quantum simulator with the spin-boson model and demonstrated its excellent agreement with the classical computer benchmark.

DOI: 10.1103/PhysRevResearch.6.013135

I. INTRODUCTION

The theory of open quantum systems offers a powerful and versatile tool to study quantum systems interacting with their external environment [1,2]. Various interesting physics have emerged along this line of investigation, including nonequilibrium phase transitions [3,4], topological and entangled state preparation by reservoir engineering [5–10], information backflow [11–16], as well as direct emulation of open quantum systems on quantum devices [17–19]. Particularly prominent playing fields of open quantum systems are the simulations of quantum dynamical processes in the condensed phase environment, and the harmonic bath with linear coupling model has served as an archetypical framework for such investigation. Intensive research efforts have been devoted to developing numerically exact computational methods based on this model to simulate open quantum system dynamics, with the non-Markovian and finite temperature effect fully accounted for. Well-established methods include quasi-adiabatic propagator path integral [20–22], hierarchical equation of motion [23–25], and multiconfiguration time-dependent Hartree [26–28]. Despite being highly successful, they all suffer exponential scaling on classical computers in one way or another. The unfavorable scaling is rooted in the fact that, in the classical computing architecture, the number of grid points used for simulating a quantum system grows exponentially with the size of the Hilbert space and the degree of non-Markovianity. Quantum computers, on the other hand, hold the promise to simulate many-body quantum dynamics in an efficient manner [29–33].

There is a growing interest in recent years in developing quantum algorithms for simulating open quantum system dynamics. However, a wealth of literature has been focused on Markovian dynamics, including the construction of universal semigroup generators [34,35], and the efficient simulation of the Lindladian [36,37] using various techniques such as block encoding [38–41], linear combination of unitaries [42], imaginary time evolution [43], and a variational approach [44]. On the other hand, quantum algorithms for non-Markovian evolution are in the nascent stage of development. Notable works include Sweke *et al.* [45] who considered locally indivisible maps that are capable of describing non-Markovian systems, and Head-Marsden *et al.* [46] who used ensembles of Lindblad trajectories originating from different times to capture the non-Markovian behavior. Recently, Wang *et al.* [47] constructed non-Markovian superoperators from the

*fwang22@gmu.edu

integrated generalized quantum master equation and implemented them on noisy intermediate-scale quantum (NISQ) devices through block encoding.

In this work, we present a quantum algorithm for simulating non-Markovian quantum dynamics based on Feynman's path integral formulation of the (multi)spin-boson Hamiltonian [48]. The system-bath interaction and the non-Markovian nature of the dynamics are captured by Feynman-Vernon's influence functional expression. This algorithm adds to the existing pool with at least three merits. First, by working with a concrete spin-boson type Hamiltonian instead of abstract maps, we expect the algorithm to be generally applicable to simulating many condensed phase quantum dynamics ranging from charge-transfer processes in solutions [49] to excitation energy transfer in a light-harvesting complex [50,51]. Secondly, all the path sums are done on the quantum machine, fully taking advantage of the quantum computer to create superposition and entanglement states, and its natural ability to represent exponentially large Hilbert space. Thirdly, the non-Markovianity is directly related to the time span of correlation function in the influence functional, and therefore the numerical convergence is straightforward (more details in Sec. III A). The following contents are organized as such. In Sec. II, we briefly present the theoretical framework of path integral formulation based on Feynman-Vernon's influence functional approach. In Sec. III, we discuss its implementation on gate-based quantum computers, including propagation scheme (Sec. III A), unitary matrix construction (Sec. III B), measurement (Sec. III C), and complexity analysis (Sec. III D). In Sec. IV, we present the simulation results with a comparison between classical and quantum computing. In Sec. V, we conclude with future work.

II. FEYNMAN'S PATH INTEGRAL

For open quantum systems, the reduced density matrix (RDM) is commonly used to investigate the dynamics. The Hamiltonian for an m-state system linearly coupled to its harmonic bath has the following expression:

$$H_s = \sum_{s=1}^{m} s|s\rangle\langle s| + \sum_{s,s'} V_{s,s'}|s\rangle\langle s'| \tag{2.1}$$

$$H_b = \sum_j \hbar\omega_j a_j^\dagger a_j, \tag{2.2}$$

$$H_{s-b} = -\sum_{s=1}^{m} s|s\rangle\langle s| \sum_j c_j \sqrt{\frac{\hbar}{2m_j\omega_j}}(a_j^\dagger + a_j), \tag{2.3}$$

where H_s and H_b denote the system and bath Hamiltonian, respectively, and H_{s-b} denotes the system-bath coupling. The system states $|s\rangle$ are usually expressed in the diabatic basis which diagonalize the position operator, and this representation fits nicely into the position representation of the path integral formulism. The coupling strength c_j and the frequency ω_j collectively define the strength-weighted density of modes called spectral density [52]:

$$J(\omega) = \frac{\pi}{2}\sum_j \frac{c_j^2}{m_j\omega_j}\delta(\omega-\omega_j). \tag{2.4}$$

The commonly used model spectral densities are of Drude or Ohmic form [2], which have a characteristic peak and a cutoff. Alternatively, the spectral density can be obtained from the Huang-Rhys factors [53] and molecular dynamics simulations [49,54,55].

The RDM in Feynman's path integral formulation is expressed as the system bare propagator multiplied by an influence functional [22]:

$$\begin{aligned}
&\rho_{\rm red}(s_N^+, s_N^-; t)\\
&= \int ds_0^+ \int ds_1^+ \cdots \int ds_{N-1}^+ \int ds_0^- \int ds_1^- \cdots \int ds_{N-1}^-\\
&\quad\times \langle s_N^+|e^{-iH_s\Delta t/\hbar}|s_{N-1}^+\rangle \cdots \langle s_1^+|e^{-iH_s\Delta t/\hbar}|s_0^+\rangle\langle s_0^+|\rho_s(0)|s_0^-\rangle\\
&\quad\times \langle s_N^+|e^{iH_s\Delta t/\hbar}|s_1^-\rangle \cdots \langle s_{N-1}^-|e^{iH_s\Delta t/\hbar}|s_N^-\rangle\\
&\quad\times I(s_0^+,\, s_1^+, ..., s_{N-1}^+,\, s_N^+,\, s_0^-,\, s_1^-, ..., s_{N-1}^-, s_N^-; \Delta t).
\end{aligned} \tag{2.5}$$

The $\{s_0^+, s_1^+, \ldots, s_N^+\}$ and $\{s_0^-, s_1^-, \ldots, s_N^-\}$ denote the discretization of the forward and backward paths, and $\langle s_0^+|\rho_0(0)|s_0^-\rangle$ is the system's initial condition. Δt is the Trotter time step.

The expression

$$I = \exp\left[-\frac{1}{\hbar}\sum_{k=0}^{N}\sum_{k'=0}^{k}(s_k^+ - s_k^-)(\alpha_{kk'}s_{k'}^+ - \alpha_{kk'}^* s_{k'}^-)\right] \tag{2.6}$$

is the influence functional, with the $\alpha_{kk'}$ coefficient (see Appendix) derived by Makri [22].

In continuous time, the $\alpha_{kk'}$ coefficient has the form

$$\alpha(t) = \frac{1}{\pi}\int_0^\infty d\omega J(\omega)\left[\coth\left(\frac{\hbar\omega\beta}{2}\right)\cos(\omega t) - i\sin(\omega t)\right], \tag{2.7}$$

which is the thermally averaged bath correlation function. This time correlation function $\alpha(t'-t'')$ is nonlocal and is responsible for the non-Markovian character of the dynamics.

Although modeling the environment's degrees of freedom using harmonic oscillators is the major assumption, the central limit theorem [54] guarantees that this type of Gaussian response is widely applicable to many condensed phase systems, and its accuracy has been demonstrated on numerous occasions [49,51,55–62].

III. QUANTUM ALGORITHM

In the following sections, we discuss in detail how Eq. (2.5) can be converted to unitary dynamics, which is preliminary for gate-based quantum computing. The major undertakings involve constructing a matrix vector multiplication scheme based on Eq. (2.5) and converting the nonunitary matrix into a unitary one. As a general feature for open quantum systems, the time evolution operator loses its unitarity due to damping and decoherence. Therefore, techniques are required to unitarize the propagator matrix, and to properly retrieve the information of the RDM through measurement.

A. Matrix vector multiplication for time propagation

The RDM can be made into a vector and represented by qubit states. As an example, for a two-level system, the vectorized RDM has the following form:

$$|\rho\rangle = \begin{pmatrix} \rho_{00} \\ \rho_{01} \\ \rho_{10} \\ \rho_{11} \end{pmatrix}, \tag{3.1}$$

where ρ_{00} and ρ_{11} are the diagonal elements of the RDM, and ρ_{01} and ρ_{10} are the off-diagonal ones. Although a general state preparation is a nontrivial task [40,63,64], for practical simulations of charge and exciton dynamics, the initial state is usually localized in one site. Therefore, the initial RDM has the form of (1,0,0,0) in the diabatic basis.

Without the influence functional, the RDM propagation in discrete time step Δt can be formulated as matrix vector multiplication:

$$\rho_s(s^{\pm}_{k+1}) = \sum_{s^{\pm}_k} K(s^{\pm}_{k+1}, s^{\pm}_k)\, \rho_s(s^{\pm}_k) \tag{3.2}$$

in which the propagator matrix $K(s^{\pm}_{k+1}, s^{\pm}_k)$ is defined as

$$K(s^{\pm}_{k+1}, s^{\pm}_k) = \langle s^{+}_{k+1}|e^{-iH_s\Delta t/\hbar}|s^{+}_k\rangle\langle s^{-}_k|e^{iH_s\Delta t/\hbar}|s^{-}_{k+1}\rangle, \tag{3.3}$$

where s_k and s_{k+1} are position states at time $t = k$ and $t = k + 1$, respectively.

The memory kernel $\alpha(t' - t'')$ in the influence functional couples timepoints further away from each other. For the condensed phase environment where the bath is composed of a broad range of frequencies, $\alpha(t' - t'')$ has a finite time span [22,65]. This observation of memory cutoff has important implications for the propagation scheme.

The matrix vector multiplication scheme complying with Eq. (2.5) has been developed by Makri [66,67] and is summarized as follows. Define $N\Delta t$ to be the memory span of the correlation function $\alpha(t' - t'')$. Propagating N time steps from the initial state, a propagator matrix T can be defined, with the matrix element shown as the following:

$$\begin{aligned} &T^{(N)}(s^{\pm}_N, \ldots, s^{\pm}_{2N-1}; s^{\pm}_0, \ldots, s^{\pm}_{N-1}) \\ &\quad = \prod_{k=0}^{N-1} K(s^{\pm}_{k+1}, s^{\pm}_k) I_0(s^{\pm}_k, s^{\pm}_k) I_1(s^{\pm}_{k+1}, s^{\pm}_k) \\ &\qquad \times I_2(s^{\pm}_{k+2}, s^{\pm}_k) \cdots I_N(s^{\pm}_{k+N}, s^{\pm}_k), \end{aligned} \tag{3.4}$$

where

$$I_j(s^{\pm}_{k'}, s^{\pm}_k) = \exp\left[-\frac{1}{\hbar}(s^{+}_{k'} - s^{-}_{k'})(\alpha_{k'k}s^{+}_k - \alpha^{*}_{k'k}s^{-}_k)\right] \tag{3.5}$$

is an element in the influence functional that dictates the coupling between two timepoints. Together, they account for the timewise self-interactions, nearest timepoint interactions, and non-nearest timepoint interactions. One subtlety is that, to match the dimensionality of the propagator matrix, the vectorized RDM has to be elongated (denoted by $\wp$), with the initial condition defined as

$$\wp(0; s^{\pm}_0, , s^{\pm}_{N-1}) = \langle s^{+}_0|\rho_s(0)|s^{-}_0\rangle. \tag{3.6}$$

For instance, for a two-state system with memory length $N = 2$, the elongated density matrix with initial condition $|\rho\rangle = (1, 0, 0, 0)$ has the form $|\wp\rangle = (1, 0, 0, 0, 1, 0, 0, 0, 1, 0, 0, 0, 1, 0, 0, 0)$. The elongated density matrix at time $t = N\Delta t$ is simply obtained through the matrix-vector multiplication,

$$\begin{aligned} &\wp(N\Delta t; s^{\pm}_N, \ldots, s^{\pm}_{2N-1}) \\ &\quad = \sum_{s^{\pm}_0, \ldots, s^{\pm}_{N-1}} T^{(N)}(s^{\pm}_N, \ldots, s^{\pm}_{2N-1}; s^{\pm}_0, \ldots, s^{\pm}_{N-1}) \\ &\qquad \times \wp(0; s^{\pm}_0, \ldots, s^{\pm}_{N-1}). \end{aligned} \tag{3.7}$$

It turns out that the propagator matrix, $T^{(N)}$, is translationally invariant in time, i.e.,

$$\begin{aligned} &T^{(N)}(s^{\pm}_N, \ldots, s^{\pm}_{2N-1}; s^{\pm}_0, \ldots, s^{\pm}_{N-1}) \\ &\quad = T^{(N)}(s^{\pm}_{k+N}, \ldots, s^{\pm}_{k+2N-1}; s^{\pm}_k, \ldots, s^{\pm}_{k+N-1}). \end{aligned} \tag{3.8}$$

Therefore, once the $T^{(N)}$ matrix is constructed for the initial time propagation, it can be reused for subsequent iterative propagation to time $t = nN\Delta t$ as

$$\wp(nN\Delta t) = \{T^{(N)}\}^n \wp(0). \tag{3.9}$$

The unique feature of this matrix vector multiplication scheme is that it does not propagate one time point to the next, but one chunk of time span of $N\Delta t$ to the next chunk. Finally, the RDM at $t = nN\Delta t \equiv L\Delta t$ is obtained by

$$\rho_s(L\Delta t; s^{\pm}_L) = \wp(L\Delta t; s^{\pm}_L; s^{\pm}_{L+1} = \cdots = s^{\pm}_{2L-1} = 0) I_0(s^{\pm}_L). \tag{3.10}$$

This completes the entire construction of the matrix vector multiplication scheme used for the time propagation of the non-Markovian quantum dynamics.

B. Unitary matrix construction

The propagator matrix $T^{(N)}$ defined in Eq. (3.4) is not a unitary matrix. This is manifested in open quantum systems where the environment exchanges energy with the system and has the decoherence effect. To convert the nonunitary matrix into a unitary one, we employ the Sz.-Nagy theorem [38,68,69], stating that a matrix T can be dilated to a unitary one by doubling its original dimension,

$$U_T = \begin{pmatrix} T & D_{T^\dagger} \\ D_T & -T^\dagger \end{pmatrix}, \tag{3.11}$$

where $D_T = \sqrt{I - T^\dagger T}$. This is possible conditioned on T being a contraction, i.e., the largest singular value of T has to be smaller or equal to 1. For a matrix that is not a contraction, it can be made contractive by rescaling it with its largest singular value. Equation (3.11) is called 1-dilation, and this block-encoding scheme requires one ancilla qubit.

If the multiplication of two nonunitary matrices T_1T_2 is desired, then the 2-dilation scheme is employed where

$$U_{T_1} = \begin{pmatrix} T_1 & 0 & D_{T_1^\dagger} \\ D_{T_1} & 0 & -T_1^\dagger \\ 0 & I & 0 \end{pmatrix}, \tag{3.12}$$

$$U_{T_2} = \begin{pmatrix} T_2 & 0 & D_{T_2^\dagger} \\ D_{T_2} & 0 & -T_2^\dagger \\ 0 & I & 0 \end{pmatrix}. \tag{3.13}$$

In general, an n-dilation matrix has the form

$$U_T = \begin{pmatrix} T & 0 & 0 & \cdots & 0 & D_{T^\dagger} \\ D_T & 0 & 0 & \cdots & 0 & -T^\dagger \\ 0 & I & 0 & \cdots & 0 & 0 \\ 0 & 0 & I & \cdots & 0 & 0 \\ \vdots & \vdots & \vdots & \ddots & \vdots & \vdots \\ 0 & 0 & 0 & \cdots & I & 0 \end{pmatrix}. \tag{3.14}$$

To propagate $T^{(N)}$ n times, n-dilation is needed. It is worth noting that since the n-dilated matrix is sparse, the compilation has polynomial scaling rather than exponential.

C. Measurement

Since the state vector for the RDM is now dilated, to obtain the information of the RDM itself, one needs to project the state vector onto its original subspace. The projection can be seen as calculating the overlap of the two wave functions, one being the state vector in the dilated space and one being the basis vectors in the original space. This overlap can be calculated on a quantum computer by the modified Hadamard test [32], shown in Figs. 1 and 2.

Here V represents the dilated propagator $T^{(N)}$, and U transforms the default computational basis to the basis of the projected subspace. For instance, for a two-state system with memory length $N = 2$, U is achieved by the Hadamard gates on the first two qubits.

D. Complexity analysis

The computational cost on classical computers scales exponentially with the memory length N. For an m-level system with memory length N, the propagator matrix has the dimension of $m^{2N} \times m^{2N}$. The space complexity (i.e., classical storage) on a classical computer is $O(m^{4N})$. For a quantum computer, the number of qubits required to store this n-dilated matrix is $\log_2 n + 2N \log_2 m$, which has exponential saving. For time complexity, the number of operations on a classical computer include $O(m^{4N})$ multiplications and $O(m^{4N})$

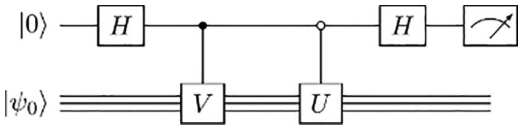

FIG. 1. Modified Hadamard test for calculating the real part of the state overlap.

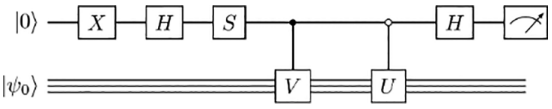

FIG. 2. Modified Hadamard test for calculating the imaginary part of the state overlap.

additions for each step of the propagation. To compile the propagator $T^{(N)}$ on a quantum machine, $d \cong 2N \log_2 m$ number of qubits are needed, which breaks down to $O(d \times 4^d)$ native gates, i.e., $O(N \log_2 m \times m^{4N})$, which scales roughly the same as on the classical machine. It is worth mentioning that this compilation complexity does not take into account the symmetry and the sparseness of the dilated propagator matrix (shown in the next section), which may reduce the gate counts to polynomial scaling.

IV. RESULTS AND DISCUSSIONS

A. System-bath parameters

We use the spin-boson model to test the quantum algorithm thus proposed. Specifically, the system Hamiltonian describes a symmetric two-level system with a nonzero off-diagonal coupling,

$$H_s = -\hbar\Omega(|s_1\rangle\langle s_2| + |s_2\rangle\langle s_1|), \tag{4.1}$$

where $|s_1\rangle$ and $|s_2\rangle$ are localized states that are eigenstates of the position operator $\hat{s}$,

$$\hat{s}|s_i\rangle = s_i|s_i\rangle, \tag{4.2}$$

and Ω is the tunneling frequency. The harmonic bath and its interaction with the system are charactered by the Ohmic spectral density,

$$J(\omega) = \frac{\pi}{2}\hbar\xi\omega e^{-\omega/\omega_c}, \tag{4.3}$$

where dimensionless ξ is the Kondo parameter that determines the strength of the system-bath coupling, and ω_c is the cutoff frequency of the bath. For all the simulation results below, the system and bath parameters are chosen to be $\Omega = 1$, $\xi = 0.1$, $\beta = 5$, $\omega_c = 7.5$, *and* $\Delta t = 0.25$, respectively. These values are chosen randomly except for the convergence parameter Δt. The values are all in atomic units.

B. Propagator matrix

The propagator matrices, T, and their dilated counterparts are demonstrated in Figs. 3–6 for memory length $N = 1$ and 2. These figures are the heat maps of the nonunitary and the dilated unitary matrices. The three plots in a row are the real, imaginary, and the absolute value of the matrix, respectively.

C. Simulation results

Three different propagation schemes are explored. The first one considers memory length $N = 1$ and is illustrated pictorially in Fig. 7 (left) where only self-interactions (loops) and nearest timepoint couplings (curves) are accounted for. They coincide with the terms $I_0(s_k^\pm, s_k^\pm)$ and $K(s_{k+1}^\pm, s_k^\pm)I_1(s_{k+1}^\pm, s_k^\pm)$

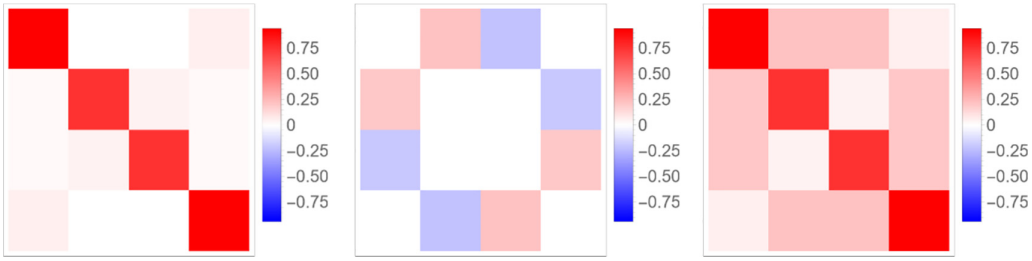

FIG. 3. Propagator matrix T with memory length $N = 1$.

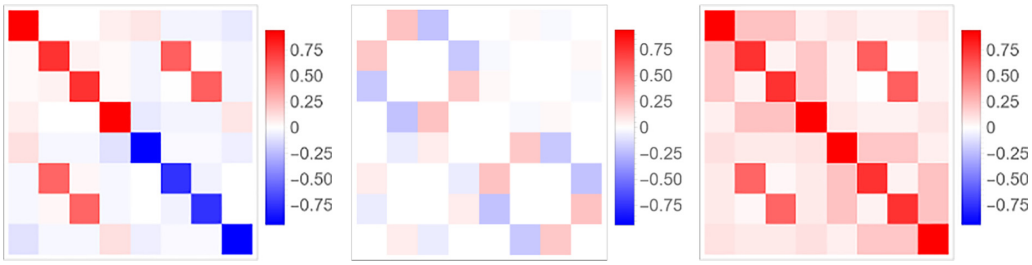

FIG. 4. Dilated propagator matrix with memory length $N = 1$.

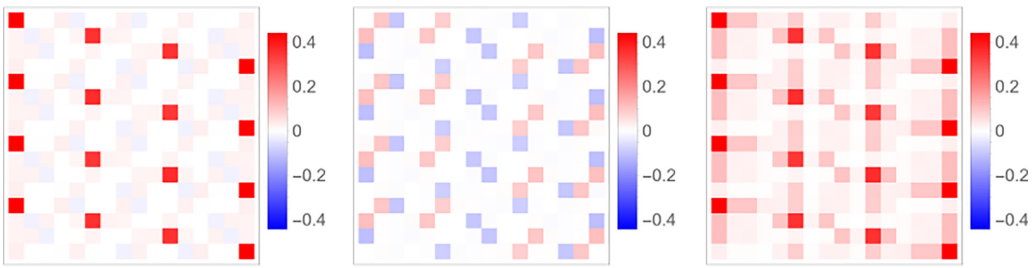

FIG. 5. Propagator matrix T with memory length $N = 2$.

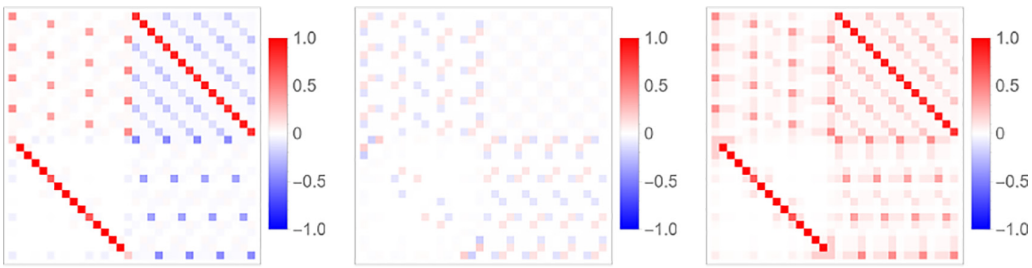

FIG. 6. Dilated propagator matrix with memory length $N = 2$.

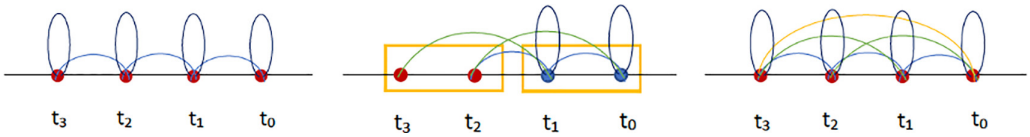

FIG. 7. Three propagation schemes. Time arrow goes from right to left. Left: $N = 1$ which includes self-interactions and nearest time couplings. Middle: Iterative scheme for $N = 2$, which includes self-interactions and nearest and non-nearest time couplings. Right: Full memory with all-time couplings.

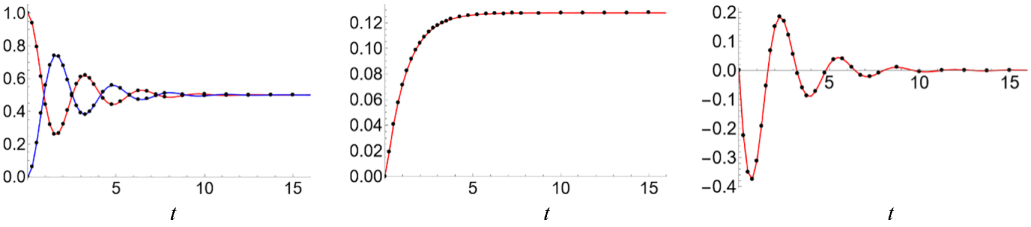

FIG. 8. Memory length $N = 1$. Left: Diagonal elements of the RDM. Middle: Real part of the off-diagonal element of the RDM. Right: Imaginary part of the off-diagonal element of the RDM. (Curves: classical benchmark; dots: quantum computing).

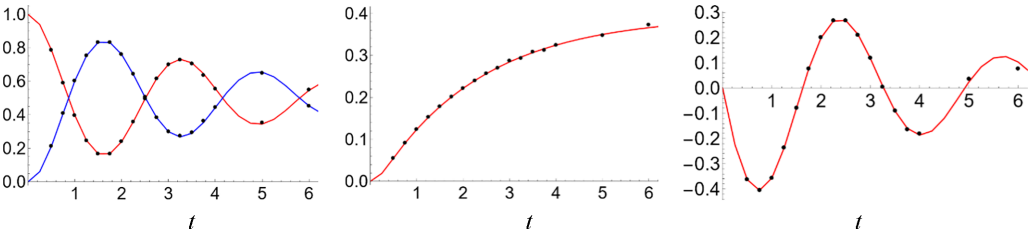

FIG. 9. Memory length $N = 2$. Left: Diagonal elements of the RDM. Middle: Real part of the off-diagonal element of the RDM. Right: Imaginary part of the off-diagonal element of the RDM. (Curves: classical benchmark; dots: quantum computing).

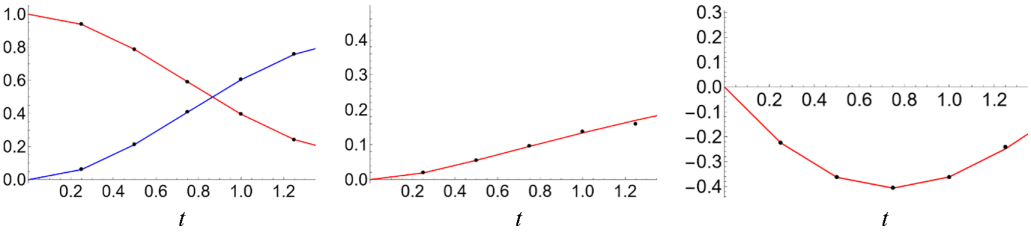

FIG. 10. Full memory. Left: Diagonal elements of the RDM. Middle: Real part of the off-diagonal element of the RDM. Right: Imaginary part of the off-diagonal element of the RDM. (Curves: classical benchmark; dots: quantum computing).

in the propagator matrix T [Eq. (3.4)]. It has the unique feature that operationally, it is Markovian, whereas, physically, it corresponds to the non-Markovian dynamics of memory span Δt. The second scheme extends to non-nearest timepoint interactions. These correspond to the I_2, I_3, … terms of the propagator matrix. As illustrated in Fig. 7 (middle) for the case of memory length $N = 2$, it iteratively propagates two timepoints to the next two timepoints. This iterative approach can be generalized for any finite memory length, and therefore deserves a separate demonstration. The third scheme explores the case where the memory spans the whole dynamics. In this scenario, full memory is included and direct implementation of the propagator matrix T without iteration is required. This propagation scheme is illustrated in Fig. 7 (right).

Figure 8–10 show the simulation results corresponding to the above three propagation schemes. Among each scheme, three plots are given that represent the diagonal elements of the RDM (population dynamics), and the real and imaginary parts of the off-diagonal elements of the RDM (coherence). The curves are benchmark calculations from the classical computer, and the dots are the quantum algorithm compiled on QISKIT [70] and simulated on QASM. Unfortunately, the depth of the circuits is too deep for NISQ devices. For all the simulations, the initial state is localized in one state. The bath is an ensemble of harmonic oscillators initially at thermal equilibrium. As the dynamics ensues, the system starts to tunnel back and forth between the two states. With time, the population eventually approaches the 50-50 equilibrium state that coincides with the detailed balance. The real and imaginary parts of the off-diagonal elements of the RDM offer information about coherence. The real part eventually approaches a fixed value that indicates the phenomenon of coherence trapping by the non-Markovian bath [71]. The quantum algorithm results match perfectly with the classical benchmark.

D. Discussions

The simulation results described thus far are non-Markovian dynamics at finite temperature. Except for the harmonic bath assumption, no other ad hoc approximations have been made. Therefore, it is expected that the algorithm can serve as a general framework for a wide range of condensed phase quantum dynamics simulations. In addition, since the memory requirement only grows linearly with the time correlation length and logarithmically with the system size, the quantum algorithm offers exponential reduction in space complexity and is well suited to handle multisite quantum dynamics, such as large spin systems in dissipative environment [72,73], or long-range proton transfer in biomolecules [74–76], which are very challenging if not impossible on classical computers.

As alluded to previously, the propagator matrices T and their dilated counterparts show very symmetric structures for a symmetric two-level system. This is due to the equivalence in time propagation between $\langle 1|T|1\rangle\langle 1|T^\dagger|1\rangle$ and $\langle 0|T|0\rangle\langle 0|T^\dagger|0\rangle$, or $\langle 0|T|1\rangle\langle 1|T^\dagger|0\rangle$ and $\langle 1|T|0\rangle\langle 0|T^\dagger|1\rangle$, etc., where the simultaneous permutations of 0 and 1 give the same results. Meanwhile, the dilated matrices are subblock sparse. Exploiting these features is expected to give more compact and shallower circuit structure [77–79] than using the existing compiling platform in QISKIT.

The novelty of our proposed algorithm can be elaborated as follows. First, it maps the temporal entanglement of the non-Markovian dynamics to the physical entanglement of the qubits, which is the root of exponential saving on memory. Second, it computes the entire path integral on the quantum machine by first encoding the path amplitude in the amplitude of the qubits and then using the Hadamard test to complete the index contraction. On the other hand, as the authors are not aware of any efficient quantum algorithm for performing singular value decomposition, there is a classical cost associated with it when constructing the dilated matrix, which scales as $O(d^3)$ for a $d \times d$ matrix.

V. CONCLUSION

We have developed a general quantum algorithm for simulating quantum dynamics of a multistate system coupled to its harmonic bath. The algorithm is based on Feynman's path integral formulation, with the influence functional accounting for the full non-Markovian effect at finite temperature. The unitary dynamics implementation is through the construction of a propagator that evolves the states spanning the full memory, and then through a block-encoding technique, the Sz.-Nagy dilation. The resource requirement scales linearly with the memory length and logarithmically with the system size and the degree of dilation, overcoming the exponential scaling on classical computers. A modified Hadamard test is used to retrieve the information of the RDM. We have demonstrated its feasibility and accuracy based on the spin-boson model on the QASM simulator. The excellent agreement between the quantum and classical computing results offers a starting point for future algorithm design for dealing with open quantum system dynamics in the finite temperature non-Markovian regime. It is important to point out that while this work has not been focused on efficient compilation, several ideas are worth exploring to render better time complexity. Such schemes include (1) quantum singular value transformation [80–82] which directly block-encodes the powers of the propagator matrix used for iteration rather than resorting to n dilation, (2) quantum imaginary time evolution [43,83] that maps the nonunitary part of the influence functional to a unitary dynamics, and (3) introducing auxiliary variables to decrease the degree of non-Markovianity [84]. These ideas are currently undergoing investigation in our group.

ACKNOWLEDGMENTS

This work is supported by National Science Foundation (NSF) under award 2320328 and the George Mason University startup fund. This work used Explore ACCESS [85] at SDSC Expanse CPU through allocation CHE220009 from the Advanced Cyberinfrastructure Coordination Ecosystem: Services and Support (ACCESS) program, which is supported by National Science Foundation Grants No. 2138259, No. 2138286, No. 2138307, No. 2137603, and No. 2138296. We would also like to thank Dr. Yiannis Loizides for the useful discussions on matrix norm, singular value, and contraction.

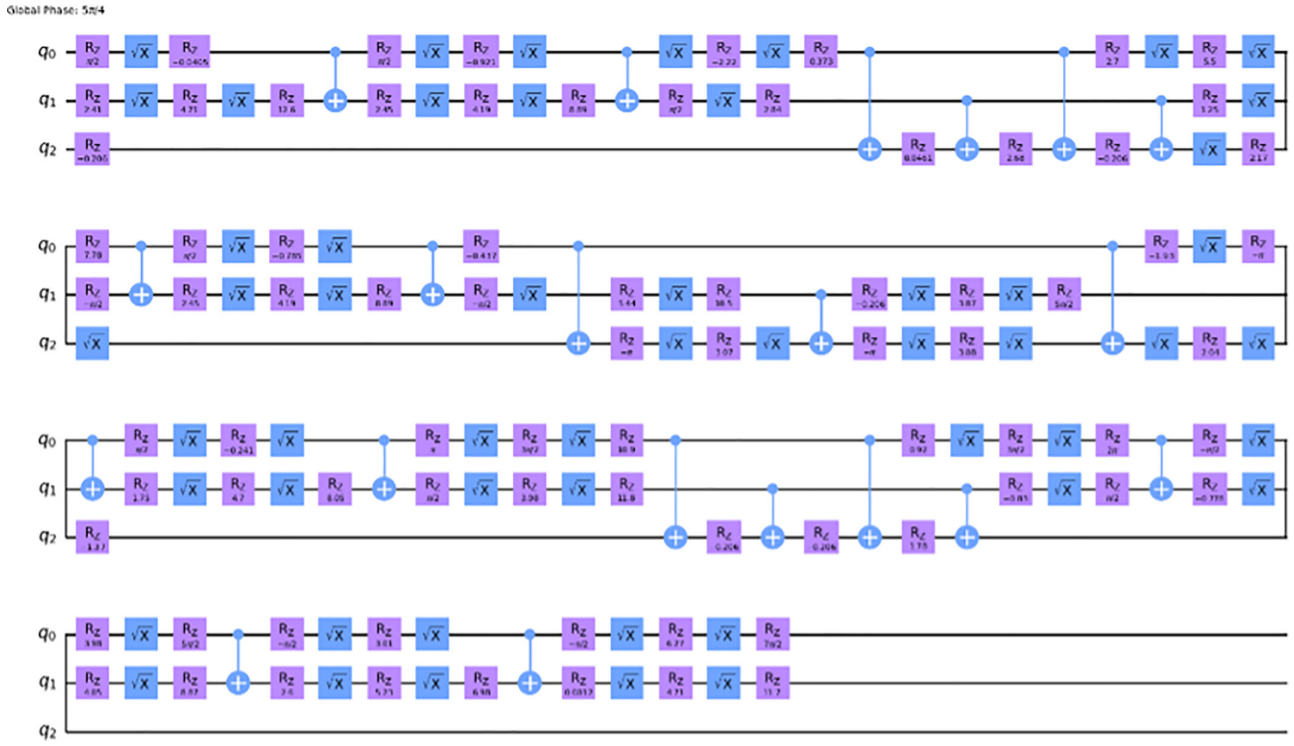

FIG. 11. Exemplar circuit for the dilate propagator matrix T with memory length $N = 1$.

APPENDIX

Below, Eqs. (A1)–(A6) are the coefficients appearing in the influence functional in Eq. (2.6).

$$\alpha_{k'k} = \frac{2}{\pi}\int_{-\infty}^{\infty} d\omega \frac{J(\omega)}{\omega^2}\frac{\exp\left(\frac{\beta\hbar\omega}{2}\right)}{\sinh\left(\frac{\beta\hbar\omega}{2}\right)}\sin^2\left(\frac{\omega\Delta t}{2}\right)e^{-i\omega\Delta t(k-k')},$$

$$0 < k < k' < N, \tag{A1}$$

$$\alpha_{kk} = \frac{1}{2\pi}\int_{-\infty}^{\infty} d\omega \frac{J(\omega)}{\omega^2}\frac{\exp\left(\frac{\beta\hbar\omega}{2}\right)}{\sinh\left(\frac{\beta\hbar\omega}{2}\right)}(1 - e^{-i\omega\Delta t}),$$

$$0 < k < N, \tag{A2}$$

$$\alpha_{N0} = \frac{2}{\pi}\int_{-\infty}^{\infty} d\omega \frac{J(\omega)}{\omega^2}\frac{\exp\left(\frac{\beta\hbar\omega}{2}\right)}{\sinh\left(\frac{\beta\hbar\omega}{2}\right)}\sin^2\left(\frac{\omega\Delta t}{4}\right)e^{-i\omega[t-(\Delta t/2)]}, \tag{A3}$$

$$\alpha_{00} = \alpha_{NN} = \frac{1}{2\pi}\int_{-\infty}^{\infty} d\omega \frac{J(\omega)}{\omega^2}\frac{\exp\left(\frac{\beta\hbar\omega}{2}\right)}{\sinh\left(\frac{\beta\hbar\omega}{2}\right)}(1 - e^{-i\omega\Delta t/2}), \tag{A4}$$

$$\alpha_{k0} = \frac{2}{\pi}\int_{-\infty}^{\infty} d\omega \frac{J(\omega)}{\omega^2}\frac{\exp\left(\frac{\beta\hbar\omega}{2}\right)}{\sinh\left(\frac{\beta\hbar\omega}{2}\right)}\sin\left(\frac{\omega\Delta t}{4}\right) \times \sin\left(\frac{\omega\Delta t}{2}\right)e^{-i\omega[k\Delta t-(\Delta t/4)]}, \quad 0 < k < N, \tag{A5}$$

$$\alpha_{Nk} = \frac{2}{\pi}\int_{-\infty}^{\infty} d\omega \frac{J(\omega)}{\omega^2}\frac{\exp\left(\frac{\beta\hbar\omega}{2}\right)}{\sinh\left(\frac{\beta\hbar\omega}{2}\right)}\sin\left(\frac{\omega\Delta t}{4}\right) \times \sin\left(\frac{\omega\Delta t}{2}\right)e^{-i\omega[t-k\Delta t-(\Delta t/4)]}, \quad 0 < k < N. \tag{A6}$$

The spectral density is extended to the negative frequencies defined as $J(-\omega) = -J(\omega)$ to avoid the singularity in the integration.

Figure 11 is an exemplar circuit for the dilate propagator matrix T.

[1] H.-P. Breuer and F. Petruccione, *The Theory of Open Quantum Systems*, 1st ed. (Oxford University Press, Oxford, 2007).
[2] U. Weiss, *Quantum Dissipative Systems*, 4th ed. (World Scientific, Singapore, 2012).
[3] I. Pižorn, One-dimensional Bose-Hubbard model far from equilibrium, Phys. Rev. A **88**, 043635 (2013).
[4] M. Jo, J. Um, and B. Kahng, Nonequilibrium phase transition in an open quantum spin system with long-range interaction, Phys. Rev. E **99**, 032131 (2019).
[5] J. C. Budich, P. Zoller, and S. Diehl, Dissipative preparation of Chern insulators, Phys. Rev. A **91**, 042117 (2015).
[6] S. Diehl, E. Rico, M. A. Baranov, and P. Zoller, Topology by dissipation in atomic quantum wires, Nat. Phys. **7**, 971 (2011).
[7] C.-E. Bardyn, M. A. Baranov, C. V. Kraus, E. Rico, A. İmamoğlu, P. Zoller, and S. Diehl, Topology by dissipation, New J. Phys. **15**, 085001 (2013).

[8] S. Diehl, A. Micheli, A. Kantian, B. Kraus, H. P. Büchler, and P. Zoller, Quantum states and phases in driven open quantum systems with cold atoms, Nat. Phys. **4**, 878 (2008).

[9] B. Kraus, H. P. Büchler, S. Diehl, A. Kantian, A. Micheli, and P. Zoller, Preparation of entangled states by quantum Markov processes, Phys. Rev. A **78**, 042307 (2008).

[10] L. Hartmann, W. Dür, and H.-J. Briegel, Steady-state entanglement in open and noisy quantum systems, Phys. Rev. A **74**, 052304 (2006).

[11] H.-P. Breuer, E.-M. Laine, and J. Piilo, Measure for the degree of non-Markovian behavior of quantum processes in open systems, Phys. Rev. Lett. **103**, 210401 (2009).

[12] Á. Rivas, S. F. Huelga, and M. B. Plenio, Entanglement and non-Markovianity of quantum evolutions, Phys. Rev. Lett. **105**, 050403 (2010).

[13] X.-M. Lu, X. Wang, and C. P. Sun, Quantum Fisher information flow and non-Markovian processes of open systems, Phys. Rev. A **82**, 042103 (2010).

[14] S. Lorenzo, F. Plastina, and M. Paternostro, Geometrical characterization of non-Markovianity, Phys. Rev. A **88**, 020102(R) (2013).

[15] B. Bylicka, D. Chruściński, and S. Maniscalco, Non-Markovianity and reservoir memory of quantum channels: A quantum information theory perspective, Sci. Rep. **4**, 5720 (2014).

[16] D. Chruściński and S. Maniscalco, Degree of non-Markovianity of quantum evolution, Phys. Rev. Lett. **112**, 120404 (2014).

[17] J. T. Barreiro, M. Müller, P. Schindler, D. Nigg, T. Monz, M. Chwalla, M. Hennrich, C. F. Roos, P. Zoller, and R. Blatt, An open-system quantum simulator with trapped ions, Nature (London) **470**, 486 (2011).

[18] A. Lemmer, C. Cormick, D. Tamascelli, T. Schaetz, S. F. Huelga, and M. B. Plenio, A trapped-ion simulator for spin-boson models with structured environments, New J. Phys. **20**, 073002 (2018).

[19] G. García-Pérez, M. A. C. Rossi, and S. Maniscalco, IBM Q experience as a versatile experimental testbed for simulating open quantum systems, npj Quantum Inf. **6**, 1 (2020).

[20] M. Topaler and N. Makri, Quasi-adiabatic propagator path integral methods. Exact quantum rate constants for condensed phase reactions, Chem. Phys. Lett. **210**, 285 (1993).

[21] M. Topaler and N. Makri, System-specific discrete variable representations for path integral calculations with quasi-adiabatic propagators, Chem. Phys. Lett. **210**, 448 (1993).

[22] N. Makri, Numerical path integral techniques for long time dynamics of quantum dissipative systems, J. Math. Phys. **36**, 2430 (1995).

[23] Y. Tanimura, Numerically "exact" approach to open quantum dynamics: The hierarchical equations of motion (HEOM), J. Chem. Phys. **153**, 020901 (2020).

[24] Y. Tanimura, Reduced hierarchical equations of motion in real and imaginary time: Correlated initial states and thermodynamic quantities, J. Chem. Phys. **141**, 044114 (2014).

[25] Y. Tanimura, Real-time and imaginary-time quantum hierarchal Fokker-Planck equations, J. Chem. Phys. **142**, 144110 (2015).

[26] M. Beck, The multiconfiguration time-dependent Hartree (MCTDH) method: A highly efficient algorithm for propagating wavepackets, Phys. Rep. **324**, 1 (2000).

[27] U. Manthe, H. -D. Meyer, and L. S. Cederbaum, Wave-packet dynamics within the multiconfiguration Hartree framework: General aspects and application to NOCl, J. Chem. Phys. **97**, 3199 (1992).

[28] H. Wang, Multilayer multiconfiguration time-dependent Hartree theory, J. Phys. Chem. A **119**, 7951 (2015).

[29] S. Somaroo, C. H. Tseng, T. F. Havel, R. Laflamme, and D. G. Cory, Quantum simulations on a quantum computer, Phys. Rev. Lett. **82**, 5381 (1999).

[30] L. Bassman Oftelie, K. Liu, A. Krishnamoorthy, T. Linker, Y. Geng, D. Shebib, S. Fukushima, F. Shimojo, R. K. Kalia, A. Nakano, and P. Vashishta, Towards simulation of the dynamics of materials on quantum computers, Phys. Rev. B **101**, 184305 (2020).

[31] A. J. Daley, I. Bloch, C. Kokail, S. Flannigan, N. Pearson, M. Troyer, and P. Zoller, Practical quantum advantage in quantum simulation, Nature (London) **607**, 667 (2022).

[32] R. Somma, G. Ortiz, J. E. Gubernatis, E. Knill, and R. Laflamme, Simulating physical phenomena by quantum networks, Phys. Rev. A **65**, 042323 (2002).

[33] A. Smith, M. S. Kim, F. Pollmann, and J. Knolle, Simulating quantum many-body dynamics on a current digital quantum computer, npj Quantum Inf. **5**, 106 (2019).

[34] D. Bacon, A. M. Childs, I. L. Chuang, J. Kempe, D. W. Leung, and X. Zhou, Universal simulation of Markovian quantum dynamics, Phys. Rev. A **64**, 062302 (2001).

[35] R. Sweke, I. Sinayskiy, D. Bernard, and F. Petruccione, Universal simulation of Markovian open quantum systems, Phys. Rev. A **91**, 062308 (2015).

[36] A. M. Childs and T. Li, Efficient simulation of sparse Markovian quantum dynamics, Quant. Inf. Comput. **17**, 901 (2016).

[37] R. Cleve and C. Wang, Efficient quantum algorithms for simulating Lindblad evolution, arXiv:1612.09512.

[38] Z. Hu, R. Xia, and S. Kais, A quantum algorithm for evolving open quantum dynamics on quantum computing devices, Sci. Rep. **10**, 3301 (2020).

[39] Z. Hu, K. Head-Marsden, D. A. Mazziotti, P. Narang, and S. Kais, A general quantum algorithm for open quantum dynamics demonstrated with the Fenna-Matthews-Olson complex, Quantum **6**, 726 (2022).

[40] A. W. Schlimgen, K. Head-Marsden, L. M. Sager-Smith, P. Narang, and D. A. Mazziotti, Quantum state preparation and nonunitary evolution with diagonal operators, Phys. Rev. A **106**, 022414 (2022).

[41] H. H. S. Chan, D. M. Ramo, and N. Fitzpatrick, Simulating non-unitary dynamics using quantum signal processing with unitary block encoding, arXiv:2303.06161.

[42] A. W. Schlimgen, K. Head-Marsden, Lee Ann M. Sager, P. Narang, and D. A. Mazziotti, Quantum simulation of open quantum systems using a unitary decomposition of operators, Phys. Rev. Lett. **127**, 270503 (2021).

[43] H. Kamakari, S.-N. Sun, M. Motta, and A. J. Minnich, Digital quantum simulation of open quantum systems using quantum imaginary–time evolution, PRX Quantum **3**, 010320 (2022).

[44] S. Endo, J. Sun, Y. Li, S. C. Benjamin, and X. Yuan, Variational quantum simulation of general processes, Phys. Rev. Lett. **125**, 010501 (2020).

[45] R. Sweke, M. Sanz, I. Sinayskiy, F. Petruccione, and E. Solano, Digital quantum simulation of many-body non-Markovian dynamics, Phys. Rev. A **94**, 022317 (2016).

[46] K. Head-Marsden, S. Krastanov, D. A. Mazziotti, and P. Narang, Capturing non-Markovian dynamics on near-term quantum computers, Phys. Rev. Res. **3**, 013182 (2021).

[47] Y. Wang, E. Mulvihill, Z. Hu, N. Lyu, S. Shivpuje, Y. Liu, M. B. Soley, E. Geva, V. S. Batista, and S. Kais, Simulating open quantum system dynamics on NISQ computers with generalized quantum master equations, J. Chem. Theory Comput. **19**, 4851 (2023).

[48] R. P. Feynman and F. L. Vernon, The theory of a general quantum system interacting with a linear dissipative system, Ann. Phys. **24**, 118 (1963).

[49] P. L. Walters and N. Makri, Quantum–classical path integral simulation of ferrocene–ferrocenium charge transfer in liquid hexane, J. Phys. Chem. Lett. **6**, 4959 (2015).

[50] A. Bose and P. L. Walters, Tensor network path integral study of dynamics in B850 LH2 ring with atomistically derived vibrations, J. Chem. Theory Comput. **18**, 4095 (2022).

[51] S. Kundu, R. Dani, and N. Makri, Tight inner ring architecture and quantum motion of nuclei enable efficient energy transfer in bacterial light harvesting, Sci. Adv. **8**, eadd0023 (2022).

[52] A. J. Leggett, S. Chakravarty, A. T. Dorsey, M. P. A. Fisher, A. Garg, and W. Zwerger, Dynamics of the dissipative two-state system, Rev. Mod. Phys. **59**, 1 (1987).

[53] M. Rätsep, Z.-L. Cai, J. R. Reimers, and A. Freiberg, Demonstration and interpretation of significant asymmetry in the low-resolution and high-resolution Q_y fluorescence and absorption spectra of bacteriochlorophyll *a*, J. Chem. Phys. **134**, 024506 (2011).

[54] N. Makri, The linear response approximation and its lowest order corrections: An influence functional approach, J. Phys. Chem. B **103**, 2823 (1999).

[55] P. L. Walters, T. C. Allen, and N. Makri, Direct determination of discrete harmonic bath parameters from molecular dynamics simulations, J. Comput. Chem. **38**, 110 (2017).

[56] S. Kundu and N. Makri, Exciton–vibration dynamics in J-aggregates of a perylene bisimide from real-time path integral calculations, J. Phys. Chem. C **125**, 201 (2021).

[57] R. A. Kuharski, J. S. Bader, D. Chandler, M. Sprik, M. L. Klein, and R. W. Impey, Molecular model for aqueous ferrous–ferric electron transfer, J. Chem. Phys. **89**, 3248 (1988).

[58] J. S. Bader and D. Chandler, Computer simulation of photochemically induced electron transfer, Chem. Phys. Lett. **157**, 501 (1989).

[59] P. L. Geissler and D. Chandler, Importance sampling and theory of nonequilibrium solvation dynamics in water, J. Chem. Phys. **113**, 9759 (2000).

[60] X. Song, D. Chandler, and R. A. Marcus, Gaussian field model of dielectric solvation dynamics, J. Phys. Chem. **100**, 11954 (1996).

[61] A. M. Barragan, A. V. Soudackov, Z. Luthey-Schulten, S. Hammes-Schiffer, K. Schulten, and I. A. Solov'yov, Theoretical description of the primary proton-coupled electron transfer reaction in the cytochrome bc_1 complex, J. Am. Chem. Soc. **143**, 715 (2021).

[62] R. E. Warburton, A. V. Soudackov, and S. Hammes-Schiffer, Theoretical modeling of electrochemical proton-coupled electron transfer, Chem. Rev. **122**, 10599 (2022).

[63] Y. R. Sanders, G. H. Low, A. Scherer, and D. W. Berry, Black-box quantum state preparation without arithmetic, Phys. Rev. Lett. **122**, 020502 (2019).

[64] M. Plesch and Č. Brukner, Quantum-state preparation with universal gate decompositions, Phys. Rev. A **83**, 032302 (2011).

[65] A. O. Caldeira and A. J. Leggett, Path integral approach to quantum Brownian motion, Phys. A: Stat. Mech. Appl. **121**, 587 (1983).

[66] N. Makri and D. E. Makarov, Tensor propagator for iterative quantum time evolution of reduced density matrices. I. Theory, J. Chem. Phys. **102**, 4600 (1995).

[67] N. Makri and D. E. Makarov, Tensor propagator for iterative quantum time evolution of reduced density matrices. II. Numerical methodology, J. Chem. Phys. **102**, 4611 (1995).

[68] H. Langer, B. Sz.-Nagy, and C. Foias, Harmonic analysis of operators on Hilbert space, Z. Angew. Math. Mech. **52**, 501 (1972).

[69] E. Levy and O. M. Shalit, Dilation theory in finite dimensions: The possible, the impossible and the unknown, Rocky Mt. J. Math. **44**, 203 (2014).

[70] H. Abraham *et al.*, QISKIT: An open-source framework for quantum computing (2019), doi:10.5281/zenodo.2562110.

[71] C. Addis, G. Brebner, P. Haikka, and S. Maniscalco, Coherence trapping and information backflow in dephasing qubits, Phys. Rev. A **89**, 024101 (2014).

[72] G. Sadiek and S. Almalki, Entanglement dynamics in Heisenberg spin chains coupled to a dissipative environment at finite temperature, Phys. Rev. A **94**, 012341 (2016).

[73] F. Hebenstreit, D. Banerjee, M. Hornung, F.-J. Jiang, F. Schranz, and U.-J. Wiese, Real-time dynamics of open quantum spin systems driven by dissipative processes, Phys. Rev. B **92**, 035116 (2015).

[74] G. A. Voth, Computer simulation of proton solvation and transport in aqueous and biomolecular systems, Acc. Chem. Res. **39**, 143 (2006).

[75] O.-H. Kwon and A. H. Zewail, Double proton transfer dynamics of model DNA base pairs in the condensed phase, Proc. Natl. Acad. Sci. USA **104**, 8703 (2007).

[76] V. R. I. Kaila, Resolving chemical dynamics in biological energy conversion: Long-range proton-coupled electron transfer in respiratory complex I, Acc. Chem. Res. **54**, 4462 (2021).

[77] M. C. Tran, Y. Su, D. Carney, and J. M. Taylor, Faster digital quantum simulation by symmetry protection, PRX Quantum **2**, 010323 (2021).

[78] M. Otten, C. L. Cortes, and S. K. Gray, Noise-resilient quantum dynamics using symmetry-preserving ansatzes, arXiv:1910.06284.

[79] K. Setia, R. Chen, J. E. Rice, A. Mezzacapo, M. Pistoia, and J. D. Whitfield, Reducing qubit requirements for quantum simulations using molecular point group symmetries, J. Chem. Theory Comput. **16**, 6091 (2020).

[80] A. Gilyén, Y. Su, G. H. Low, and N. Wiebe, Quantum singular value transformation and beyond: Exponential improvements for quantum matrix arithmetics, in *Proceedings of the 51st Annual ACM SIGACT Symposium on Theory of Computing* (ACM, Phoenix, 2019), pp. 193–204.

[81] G. H. Low and I. L. Chuang, Optimal Hamiltonian simulation by quantum signal processing, Phys. Rev. Lett. **118**, 010501 (2017).

[82] J. M. Martyn, Z. M. Rossi, A. K. Tan, and I. L. Chuang, Grand unification of quantum algorithms, PRX Quantum **2**, 040203 (2021).

[83] M. Motta, C. Sun, A. T. K. Tan, M. J. O'Rourke, E. Ye, A. J. Minnich, F. G. S. L. Brandão, and G. K.-L. Chan, Determining eigenstates and thermal states on a quantum computer using quantum imaginary time evolution, Nat. Phys. **16**, 205 (2020).

[84] T. Banerjee and N. Makri, Quantum-classical path integral with self-consistent solvent-driven reference propagators, J. Phys. Chem. B **117**, 13357 (2013).

[85] T. J. Boerner, S. Deems, T. R. Furlani, S. L. Knuth, and J. Towns, ACCESS: Advancing Innovation: NSF's Advanced Cyberinfrastructure Coordination Ecosystem: Services & Support, in *Practice and Experience in Advanced Research Computing* (ACM, Portland OR USA, 2023), pp. 173–176.